

Stability of Continuous Time Quantum Walks in Complex Networks

Adithya L J^{1,2}, Johannes Nokkala^{3,4}, Jyrki Piilo³,
Chandrakala Meena^{1,2*}

¹Department of Physics, Indian Institute of Science Education and Research, Street, Pune, 411008, India.

²School of Physics, Indian Institute of Science Education and Research Thiruvananthapuram, 695551, Kerala, India.

³Department of Physics and Astronomy, University of Turku, FI-20014 Turun yliopisto, State, Finland.

⁴Turku Collegium for Science, Medicine and Technology, University of Turku, Turku, Finland.

*Corresponding author(s). E-mail(s): meenachandrakala@gmail.com;
Contributing authors: adiethu@gmail.com; jsinok@utu.fi;
jyrki.piilo@utu.fi;

Abstract

We investigate the stability of continuous-time quantum walks (CTQWs) in a range of network topologies under different decoherence mechanisms, defining stability as the system's ability to preserve quantum properties over time. The networks studied range from homogeneous to heterogeneous structures, including cycle, complete, Erdős–Rényi, small-world, scale-free, and star topologies. The decoherence models considered are intrinsic decoherence, Haken–Strobl noise, and quantum stochastic walks (QSWs). To assess quantum stability, we employ several metrics: node occupation probabilities, the ℓ_1 -norm of coherence, fidelity with the initial state, quantum-classical distance, and von Neumann entropy. Our results reveal that the interplay of both network topology and decoherence model influences coherence preservation. Intrinsic decoherence results in the slowest decay of coherence, followed by Haken–Strobl noise, while QSW causes the most rapid loss of coherence. The stability ranking among network topologies varies depending on the decoherence model and quantifier used. For example, under Haken–Strobl and intrinsic decoherence, the quantum-classical distance ranks the cycle network more stable than scale-free networks, although other

metrics consistently favour scale-free topologies. In general, heterogeneous networks, such as star and scale-free networks, exhibit the highest stability, whereas homogeneous topologies, such as cycle and Erdős–Rényi networks, are more vulnerable to decoherence. The complete graph, despite its homogeneity, remains highly stable due to its dense connectivity. Furthermore, in heterogeneous networks, the centrality of the initialized node, measured by degree or closeness, has a pronounced impact on stability, underscoring the role of local topological features in quantum dynamics.

Keywords: Continuous-time Quantum Walks, Complex Networks, Decoherence Dynamics, Quantum Coherence, Quantum Stability

1 Introduction

Quantum walks (QWs), the quantum analogs of classical random walks, have emerged as a powerful framework for exploring a wide range of quantum phenomena, including quantum computation, coherent transport, and the dynamical behavior of complex quantum systems [1–3]. Unlike their classical counterparts, QWs exploit quantum superposition and interference, enabling the walker to explore graphs more efficiently and, in some cases, achieve quantum speedups in algorithmic tasks [4].

QWs can be broadly categorized into two types: discrete-time quantum walks (DTQWs) [1] and continuous-time quantum walks (CTQWs) [5]. DTQWs evolve via alternating applications of a coin operator and a conditional shift, allowing fine-grained control over the walker’s trajectory [6]. This approach has proven useful in quantum search algorithms [7] and in simulating topologically nontrivial phases [8]. In contrast, CTQWs evolve under a time-independent Hamiltonian defined by the graph structure, without requiring an internal coin degree of freedom. This formulation is particularly well-suited for modeling coherent transport in structured networks and has applications in quantum search [4, 9, 10], quantum state transfer [11], entanglement routing [12], and energy transport in photosynthetic complexes [13].

However, real-world implementations of QWs are inevitably affected by decoherence arising from environmental interactions and imperfections in the system. These effects disrupt unitary evolution, suppress quantum coherence, and reduce transport efficiency and computational fidelity [14, 15]. Interestingly, in some cases decoherence can also assist transport [16, 17]. Understanding how decoherence influences QWs is therefore critical for the development of robust quantum technologies.

Since decoherence in open quantum systems is typically continuous rather than discrete [14], our study focuses on CTQWs under a variety of continuous decoherence mechanisms. Common modeling approaches include intrinsic decoherence, modeled as dephasing in the energy eigenbasis via the Milburn equation [18]; position-basis decoherence, described by the Haken–Strobl master equation [19]; and quantum stochastic walks (QSW), which interpolate between quantum and classical regimes [20]. These frameworks thus enable us to explore different facets of open quantum dynamics and their consequences for quantum transport.

The evolution of CTQWs is influenced by both the form of decoherence and the structure of the underlying graph [21, 22]. Earlier studies have explored CTQW dynamics on one-dimensional lattices to examine quantum transport [23] and quantum correlations [24], while more recent efforts have extended this work to symmetric and complex networks, assessing how structure interacts with decoherence [21, 25, 26].

In this work, we broaden the scope by considering a diverse set of network topologies, from homogeneous to highly heterogeneous, and evaluating their behavior under multiple decoherence models. Our primary objective is to understand how the interplay between network structure and environmental noise governs the behavior and stability of CTQWs.

Motivated by analogous findings in classical network theory, where the stability of dynamical states is often determined by the interplay between topology and dynamics [25, 27, 28], so in this study we seek to uncover similar principles within the context of quantum systems. Specifically, we investigate how the CTQW dynamics evolves under various decoherence mechanisms across different network architectures. Here, we define quantum stability as the ability of a system to retain its quantum features, such as coherence, over time despite the presence of decoherence.

It is well established that node's centralities, such as degree, betweenness, and closeness, play a critical role in determining the resilience of classical networks [29, 30]. Recent studies indicate that these structural attributes also significantly influence quantum dynamics [31]. Identifying which topological features help mitigate or exacerbate decoherence is essential for designing stable and efficient quantum systems. Such insights are crucial for advancing robust quantum communication protocols, quantum devices, and fault-tolerant quantum architectures [32]. Motivated by this, our study also investigates how node centralities affect quantum stability, with a particular focus on heterogeneous networks, where centrality disparities are pronounced. To quantify the stability of CTQWs under different decoherence models, we employ several metrics commonly used in the analysis of open quantum systems, including quantum-classical distance, von Neumann entropy, ℓ_1 -norm of coherence, and fidelity. These measures provide a multifaceted view of how far the system deviates from ideal quantum behavior over time. For example, the quantum-classical distance has been used to study how CTQWs diverge from quantum behavior under decoherence in simple network topologies such as complete, cycle, and star graphs [21].

Building on this foundation, we extend the analysis to more complex graphs and a broader range of decoherence mechanisms. Specifically, this study investigates how different forms of decoherence affect the resilience of CTQWs across both simple and complex network structures. Our results provide insights into open quantum dynamics on networks and offer guidance for designing quantum systems that maintain coherence in the presence of environmental disturbances.

We begin Sec. 2 by detailing the dynamics of CTQWs in the presence of various decoherence mechanisms. In Sec. 3, we provide an overview of the network structures considered in our study. Sec. 4 introduces the quantitative measures employed to assess the stability of CTQWs across different graph topologies. The primary findings of our investigation are presented in Sec. 5, where we analyze how decoherence impacts

quantum transport on both simple and complex networks. Finally, Sec. 6 concludes the paper with a summary of our key results and their broader implications.

2 Dynamical framework of quantum networks

In a CTQW on a network, the walker is initially localized at a specific node and gradually explores the network as time evolves. The evolution of the quantum state is governed by a Hamiltonian, typically chosen to be the graph Laplacian of the underlying network.

The Laplacian matrix is defined as $L = D - A$, where D is the diagonal degree matrix with the degree (i.e., number of connections) of each node as its diagonal elements, and A is the adjacency matrix, with elements $A_{ij} = 1$ if node i and j are connected and $A_{ij} = 0$ otherwise.

We investigate the impact of three distinct types of decoherence on CTQW: (i) intrinsic decoherence, modeled by the Milburn equation [18], (ii) position-basis decoherence, described by the Haken–Strobl master equation [19], and (iii) quantum stochastic walks, as formulated in [20]. Each of these models introduces a unique form of non-unitary evolution, enabling us to explore different facets of quantum system dynamics under decoherence on networks.

In the absence of decoherence, that is, ideal noiseless conditions, the quantum walker evolves coherently, governed by unitary dynamics. This evolution is described by the Liouville–von Neumann equation [33]:

$$\frac{d\rho(t)}{dt} = -i[H, \rho(t)]. \quad (1)$$

Where $\rho(t)$ denotes the density matrix of the system at time t , and H is the system’s Hamiltonian, typically chosen as the graph Laplacian L in the context of network-based quantum walks.

To model intrinsic decoherence, we take Milburn formalism [18], which introduces non-unitary dynamics by modifying the noiseless evolution Eq. (1) as follows:

$$\frac{d\rho(t)}{dt} = -i[H, \rho(t)] - \frac{\gamma}{2}[H, [H, \rho(t)]]. \quad (2)$$

Here, γ represents the decoherence rate. This model captures intrinsic decoherence, which reflects the system’s internal loss of coherence, independent of external environmental interactions. In our simulations, we set $\gamma = 0.1$ without loss of generality, following [21]. This value introduces reasonable decoherence effects while preserving essential features of quantum dynamics. The double-commuter term in Eq. (2) models loss of coherence in the energy basis.

The next model we consider is based on the Haken–Strobl master equation, which is commonly employed to describe dephasing noise on the position basis. It takes the following form [19]:

$$\frac{d\rho(t)}{dt} = -i[H, \rho(t)] + \gamma \sum_k \left(P_k \rho(t) P_k^\dagger - \frac{1}{2} \{P_k^\dagger P_k, \rho(t)\} \right); \quad (3)$$

$P_k = |k\rangle\langle k|$ are projectors on the position basis. This equation models decoherence by coupling the system to a bath that causes loss of coherence between different positions without energy exchange.

The last decoherence model is Quantum Stochastic Walk (QSW) [20] that interpolates between pure quantum and classical behavior. It is described by the Gorini–Kossakowski–Sudarshan–Lindblad master equation [34–36] as follows:

$$\begin{aligned} \frac{d\rho(t)}{dt} = & - (1 - p)i[H, \rho(t)] \\ & + p \sum_{kj} \left(P_{kj}\rho(t)P_{kj}^\dagger - \frac{1}{2} \left\{ P_{kj}^\dagger P_{kj}, \rho(t) \right\} \right); \end{aligned} \quad (4)$$

$P_{kj} = L_{kj}|k\rangle\langle j|$ and p is the parameter that controls the interpolation between unitary evolution and stochastic noise. We consider $p = 0.1$, which corresponds to small decoherence, but previous studies [21] have shown that it is enough to study the effect of quantum stochastic decoherence.

3 Network Topologies

We consider a quantum walker evolving under CTQW dynamics, where the walker is initially localized at a single node in the network. This approach is applied consistently across all the networks that we consider in this study. The rationale behind this choice is to minimize the fidelity between the quantum-evolved state and the classically evolved state, as discussed in prior studies on CTQW [37]. As the system evolves, the walker’s state becomes a quantum superposition over multiple nodes, with the probability of finding the walker at a given node determined by the diagonal terms of the density matrix.

As a baseline for comparison with more complex networks, we begin our analysis with three simple graph structures: complete, cycle, and star graphs, each have a size of node number $N = 10$.

In a complete graph, every node is connected to all other nodes, resulting in a homogeneous network, where each node has degree of $N - 1$. The cycle graph is also a homogeneous network, where each node is connected only to its two nearest neighbors, yielding a uniform degree of 2. In contrast, the star graph exhibits a highly heterogeneous structure in which the central hub node has degree $N - 1$, while all peripheral (edge) nodes are connected only to the center node and hence have degree 1.

We consider three types of complex network topologies for our simulations: Barabási–Albert scale-free networks [38], Erdős–Rényi random networks [39], and Watts–Strogatz small-world networks [40], as illustrated in Fig. 1. These network models differ significantly in their structural characteristics due to distinct connectivity patterns.

Erdős–Rényi networks [39] are homogeneous, with a binomial degree distribution tightly centered around the average degree, making the nodes statistically similar in connectivity. In contrast, Barabási–Albert networks [38] are scale-free, characterized

by a power-law degree distribution. This results in a few highly connected hub nodes, introducing significant degree heterogeneity into the network.

The Watts–Strogatz model [40] generates small-world networks with high clustering and short average path lengths. Starting from a regular ring lattice where each node is connected to its four nearest neighbors, a small fraction of the edges is randomly rewired with probability $p = 0.1$, introducing long-range shortcuts while maintaining local structure [41]. This process disrupts the periodicity of the lattice, creating a network that is partially random but still relatively homogeneous in degree distribution.

Thus, the scale-free network is the most heterogeneous due to the presence of hubs, the Erdős–Rényi network is the most homogeneous, and the small-world network lies in between, with a regular structure perturbed by some randomness. For all simulations involving these network topologies, we consider networks of size $N = 100$ nodes, each with an average degree of 4.

4 Stability of quantum networks

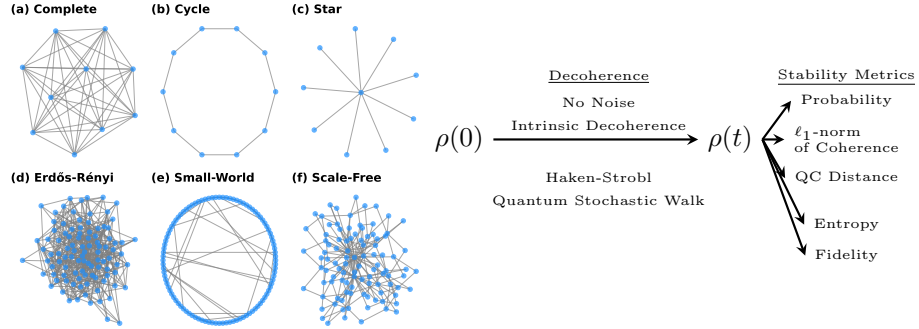


Fig. 1 Schematic diagram for determining quantum stability. To determine the stability of the quantum walker which is initially localized on a specific node of a graph topology and evolves over time. The evolution of the walker depends on the type of decoherence and the network topology. The stability analysis is performed using probability distribution, coherence ℓ_1 -norm, fidelity with initial state, von Neumann entropy, and quantum-classical distance.

To investigate the stability of CTQWs on networks under decoherence, we analyze several quantities for example, the occupation probability of the walker across nodes, the ℓ_1 -norm of coherence, the fidelity with respect to the initial state, the von Neumann entropy, and the quantum–classical distance, as illustrated in Fig. 1. These metrics are complementary, each capturing distinct aspects of the system’s behavior and collectively providing a comprehensive picture of stability under decoherence. The following subsections provide brief descriptions of each of these measures.

4.1 Occupation Probability

We analyze the node occupation probability and its long-time behavior to understand the influence of decoherence on CTQWs. The occupation probabilities corresponds to the diagonal elements of the density matrix. In the presence of decoherence, the occupation probability evolves toward a steady state over time. The rate at which the system approaches its steady state serves as an informative measure of the CTQW's stability in the presence of decoherence. Slower convergence reflects greater stability of the CTQW under specific decoherence. Moreover, when the occupation probabilities approach uniformity across nodes, the system tends toward classical-like behavior, signaling a transition from quantum to classical [25].

4.2 ℓ_1 -norm of coherence

ℓ_1 -norm of coherence is the sum of the absolute values of all off-diagonal elements of the density matrix [42].

$$C_{\ell_1}(\rho(t)) = \sum_{i \neq j} |\rho_{ij}(t)|. \quad (5)$$

Decay of the ℓ_1 -norm of coherence toward zero signifies the gradual loss of coherence, indicating that the system is undergoing classicalization under the given decoherence mechanism. In contrast, if a non-negligible level of coherence is maintained over time, the CTQW retains its quantum character and can be considered as stable.

4.3 Fidelity

Fidelity [43–46] quantifies the degree of overlap between the initial quantum state and the state evolved under decoherence. It measures how closely the evolved state overlaps to the initial state. Given the density matrix $\rho(t)$ at time t and the initial density matrix ρ_0 , the fidelity F is defined:

$$F(\rho_0, \rho(t)) = \left[\text{Tr} \left(\sqrt{\sqrt{\rho_0} \rho(t) \sqrt{\rho_0}} \right) \right]^2. \quad (6)$$

Higher fidelity indicates that the quantum state retains more of its initial state over time, reflecting that the quantum walker is more localized to the initial state which is not expected in classical scenario.

4.4 Von Neumann Entropy

Von Neumann entropy measures the degree of mixedness of the quantum state as a result of decoherence [47]. It is defined as:

$$S(\rho(t)) = -\text{Tr}(\rho(t) \log \rho(t)). \quad (7)$$

This entropy quantifies the loss of coherence in the quantum state due to interaction with the environment, indicating how much the state has deviated from a pure quantum state towards a mixed state. High entropy indicates a more mixed quantum state due to decoherence, while low entropy reflects a purer quantum state. When there is no noise entropy will stay zero.

4.5 Quantum-Classical Distance

The quantum-classical distance $D_{QC}(t)$ measures the deviation between the quantum evolution and the classical evolution of the system [37]. It is defined as:

$$D_{QC}(t) = 1 - \min_{\rho_0} F(\rho_{Cl}(t), \rho_Q(t)), \quad (8)$$

where F represents the fidelity between the classical and quantum density matrices. The classical density matrix $\rho_{Cl}(t)$ is given by:

$$\rho_{Cl}(t) = \sum_{k=1}^N p_{kj}(t) |k\rangle\langle k|, \quad (9)$$

with $p_{kj}(t)$ denoting the classical transition probability from node j to node k :

$$p_{kj}(t) = \langle k | e^{-Lt} | j \rangle. \quad (10)$$

The quantum-classical distance is a measure that tells the divergence between quantum and classical evolution. If it is 0, then the quantum evolution is fully classicalized, which is not desired, and if 1, where the system evolves entirely different from classical evolution, indicates that decoherence has not classicalized the system and quantum properties are preserved. Quantum classical distance for complete cycle and star topologies is already studied in [21].

Using these metrics on different topologies, we analyze which topology is more preferred under different decoherences.

5 Results

5.1 CTQW on Complete, Cycle and Star Networks

To investigate the evolution of the CTQW on various network topologies, we first study the triangle network and compare its node occupation probabilities with the analytical results provided in Appendix A (see Fig. 9). We then examine the dynamics on simple networks such as the cycle, complete, and star topologies, as shown in Fig. 2. Star networks consists of two types of nodes: peripheral nodes, each with degree 1, and a central hub node with degree $N - 1$, so for this network, we consider two distinct initial conditions: in the first case, the walker is localized at the central hub node, and in the second case, it is initialized on one of the peripheral nodes. In contrast, both cycle and complete networks consist of nodes of uniform degree. Therefore, for these topologies, the CTQW is initially located on a randomly selected node due to the symmetry of the graph. In all the cases, the initially localized node refers to the node with probability 1 at the initial time step illustrated in Fig. 2.

In the absence of noise, the CTQW on the cycle network as shown in Fig. 2(a), explores not only the initially localized node but also other nodes in the network. In contrast, for both the star and complete network topologies, the CTQW tends to remain localized near the initially occupied node, maintaining a high occupation probability at that node, as illustrated in Fig. 2(b)–(d). Moreover, the probability oscillations in the complete graph and the star network with hub node initialization

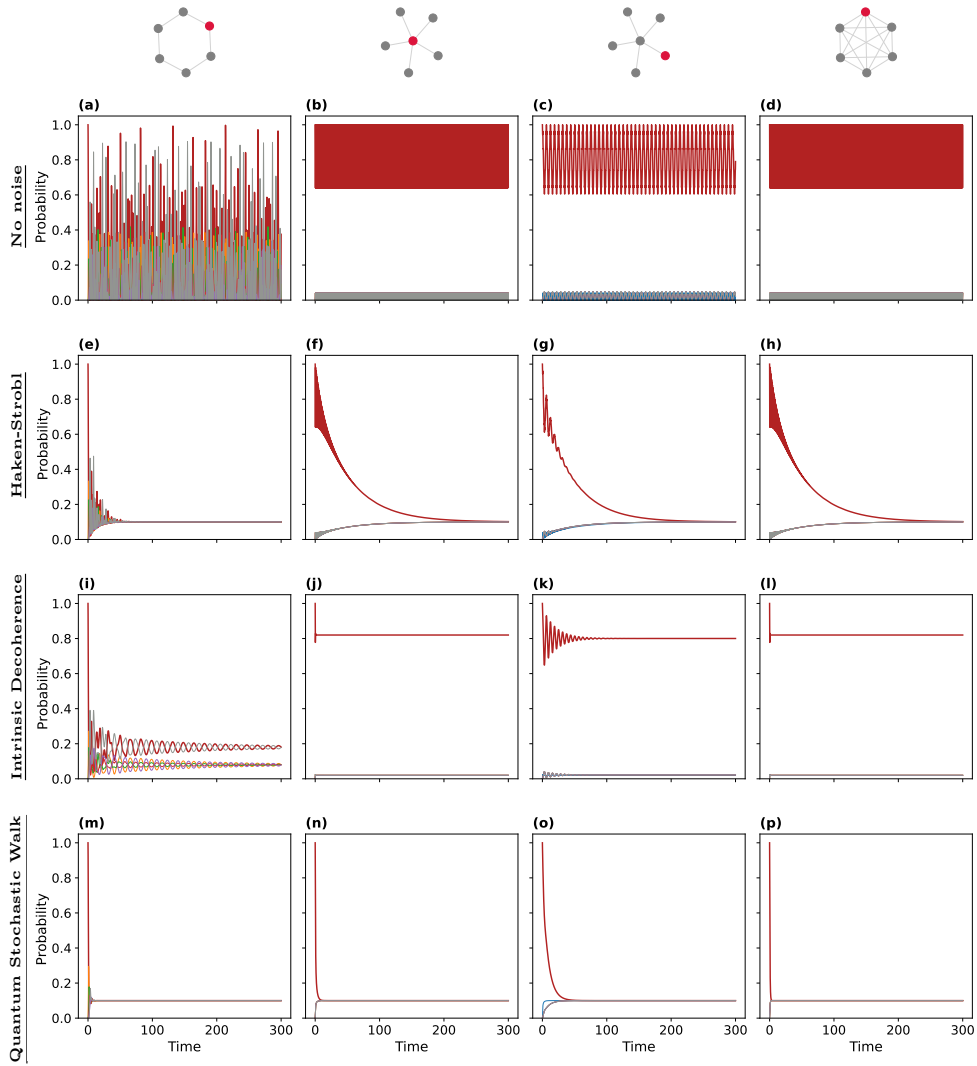


Fig. 2 Probability distribution of the CTQW on some simple network topologies with network size $N = 10$. To examine the probability distribution of CTQW on various network structures, we consider three representative topologies: cycle, star, and complete graphs, each consisting of $N = 10$ nodes. In each network, the red-colored node indicates the site where the walker is initially localized with probability 1 at time $t = 0$. The temporal evolution of the probability distribution is illustrated under four scenarios: (a)–(d) the noiseless case, (e)–(h) Haken–Strobl noise, (i)–(l) intrinsic decoherence, and (m)–(p) QSW. The four columns correspond to the different network configurations: cycle (first column), star with hub node initialization (second column), star with peripheral node initialization (third column), and complete graph (fourth column).

exhibit a higher frequency compared to the star network with peripheral node initialization. For the star network with initial localization at a peripheral node in Fig. 3(c), the ℓ_1 -norm of coherence oscillates with lower frequency compared to the cases of the star with central node initialization and the complete graph, both of which show similar and more rapid oscillatory behavior as shown in Fig. 3(b),(d). This observation is consistent with previous findings by Xu et al. [48], who showed that transition probabilities are high-frequency revivals in the case of hub node excitation, along with strong long-term localization at the initial site for the star network. In addition to it, that study also demonstrated that the transport dynamics on a star graph with hub node excitation are equivalent to those on a complete graph of the same size. In contrast, for the cycle network, the ℓ_1 -norm of coherence displays fluctuations that do not go to zero, as shown in Fig. 3(a) and it exhibits a higher coherence, as measured by the ℓ_1 -norm of coherence, than both the complete and star networks. This can be attributed to the absence of high-degree nodes in the cycle network, which allows for delocalized dynamics and a higher value of coherence. These observations suggest that the dynamics of CTQW are highly sensitive to both the underlying network structure and the choice of initial localization.

Under Haken–Strobl noise, the occupation probabilities of the CTQW on the cycle graph as shown in Fig. 2(e) converge to a uniform distribution significantly faster than on the other topologies given in Fig. 2(f)-(h), indicating rapid delocalization and the onset of a steady state. This behavior resembles the equilibration of probabilities observed in classical continuous-time random walks [25]. The quantum coherence, quantified by the ℓ_1 -norm of coherence, also decays much more rapidly on the cycle topology as shown in Fig. 3(a) compared to the star and complete networks in Fig. 3(b)-(d). To determine the rate of coherence loss, we fitted the simulated coherence data using the stretched exponential Kohlrausch function [49]:

$$C(t) = C_0 \exp(-(\lambda t)^\beta). \quad (11)$$

Here, λ is the effective decay rate that determines how quickly the function decreases(increases) over time, while β is the stretching exponent that characterizes the nature of the decay. A value of $\beta = 1$ corresponds to standard exponential decay, whereas $\beta < 1$ coherence decay slower than exponential decay and for $\beta > 1$ the quantum walker loses coherence faster than exponential decay. However, the overall behavior of the coherence decay is determined by the combined influence of both λ and β . We fitted coherence data obtained for the Haken-Strobel and quantum stochastic decoherences as shown in Fig. 3(e),(f),(g),(h) and the extracted coefficients λ and β , summarized in Table 1. These extracted coefficients λ and β , further support our observations: the star network with the central node as the initial localization and the complete network exhibit slower coherence decay, indicating greater robustness against Haken–Strobl decoherence compared to both the cycle network and the star network initialized at a peripheral node. These findings conclude that, under Haken–Strobl noise, the star network initialized at a hub node and the complete network are more resilient in preserving quantum coherence than the cycle network and the star network initialized at the central node. Among all the network configurations considered, the cycle network performs the worst in maintaining quantum coherence for a long time

and the star network with peripheral node initialization in a short time. However, it should be noted that for Haken-Strobl decoherence, all network topologies exhibit $\beta < 1$ as in Table 1, indicating that the decay of coherence is slower than exponential in all cases.

Decoherence	Network	λ	β
Haken-Strobl	Cycle	0.14	0.86
	Star Hub	0.03	0.90
	Star peripheral	0.10	0.71
	Complete	0.03	0.90
Quantum Stochastic	Cycle	0.08	2.03
	Star Centre	0.28	2.62
	Star peripheral	0.06	1.23
	Complete	2.00	1.00

Table 1 Coherence decay fitting parameters for cycle, star, and complete networks under Haken-Strobl and QSW.

The evolution of CTQW under intrinsic decoherence is shown in Fig. 2(i)-(l), respectively, on cycle, star, and complete networks. From these figures, we observe distinct differences in the localization behavior, for instance, on star and complete topologies, CTQW tends to remain localized with a significantly high probability at the initial node compare than at other nodes in the network. In contrast, for the cycle topology, although the probabilities do not become exactly uniform, there is no strong localization on the initially localized node, unlike in star and complete topologies. Instead, the occupation probabilities of different nodes exhibit persistent oscillations over time (see Fig. 2(i)). As shown in Fig. 3(a)-(d) across all network types, coherence under intrinsic decoherence is preserved to varying extents. In the cycle network, the ℓ_1 -norm of coherence exhibits temporal fluctuations even at large times. For the star network with initial localization at a peripheral node, coherence exhibits damped oscillations before settling into a steady state value. Interestingly, for both the complete network and the star network with central hub node initialization, the coherence also converges to the same steady state value observed in the peripheral initialization case. Although the cycle network retains some coherence under intrinsic decoherence, the level of preservation is lower compared to the star and complete topologies. Notably, the cycle exhibits oscillatory behavior in both probability and coherence dynamics under intrinsic decoherence, a feature that is absent in the star and complete networks.

In the case of QSW decoherence, the decay of coherence is faster for complete network than other topologies. However, decay of coherence under QSW decoherence is much faster than Haken-Strobl for all network topologies, as shown in Table 1. Star graph with peripheral node initialization takes longer to reach the same probability distribution and exhibits a slower decay of coherence compared to other topologies and the star graph with center initialization, as seen in Fig. 2(m)-(p) and Fig. 3(e)-(h). This observation is further supported by exponents λ and β as shown in Table 1, which shows that the coherence takes a longer time to decay in the star topology

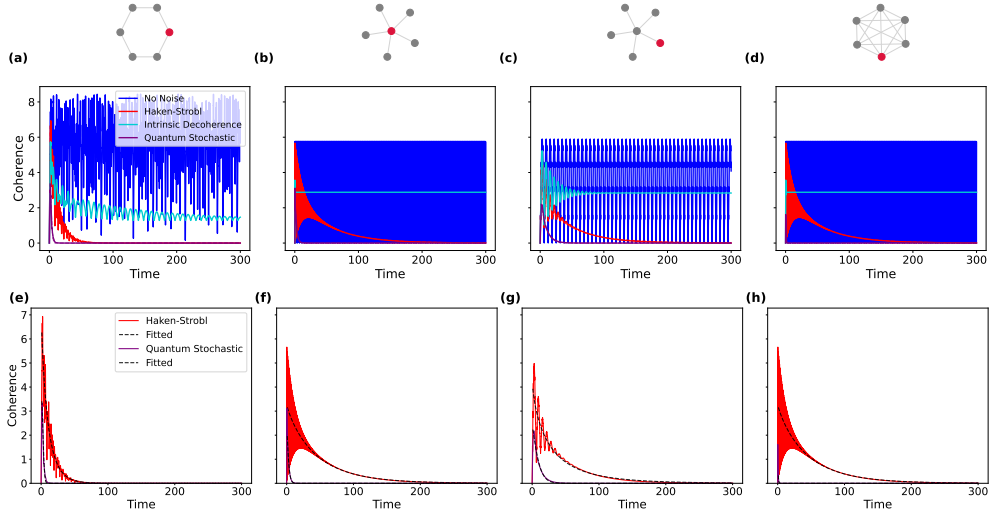


Fig. 3 ℓ_1 -norm of coherence with time for simple topologies with network size $N = 10$. In the first row, ℓ_1 -norm of coherence is plotted for all types of decoherence for cycle (a), star network with hub node initialization (b) and peripheral node initialization (c), and complete network (d). The second row presents the coherence decay profiles for both Haken–Strobl noise and QSW, with the data fitted using the proposed decay model in Eq. (11), with the best-fit parameters summarized in Table 1.

than cycle and complete topologies, indicating greater stability of this topology under QSW induced decoherence.

The behavior of quantum-classical distance, fidelity with the initial state, and von Neumann entropy is presented in Appendix B for networks of size $N = 50$ in Fig. 12 and Fig. 13, and for networks of size $N = 10$ in Fig. 10 and Fig. 11. The $N = 50$ results are particularly informative, clearly distinguishing the relative stability of different topologies. Under Haken–Strobl noise and intrinsic decoherence, the star network (with hub node initialization) and the complete graph exhibit high stability, indicated by elevated quantum-classical distances and fidelities, along with low entropy. For the QSW, the star network initialized at a peripheral node shows improved stability, as seen from its high fidelity and low entropy. Interestingly, the quantum-classical distance highlights the cycle network as especially robust against classicalization.

5.2 CTQW on Complex Network Topologies

To further validate our observations, we extend our analysis to more complex topologies to investigate how different network structures influence the stability of quantum systems. Specifically, we study the evolution of CTQW on Erdős–Rényi, small-world, and scale-free networks. As the degree of the initially localized node can significantly affect the dynamics, we choose a high-degree node as the initial localization in the heterogeneous scale-free network. In contrast, the Erdős–Rényi and small-world networks have nodes with approximately similar average degrees, so the impact of the initial node selection is expected to be comparatively minimal in these cases. In all

cases, the initially localized node is defined as the node with probability 1 at the initial time step (see Fig. 4).

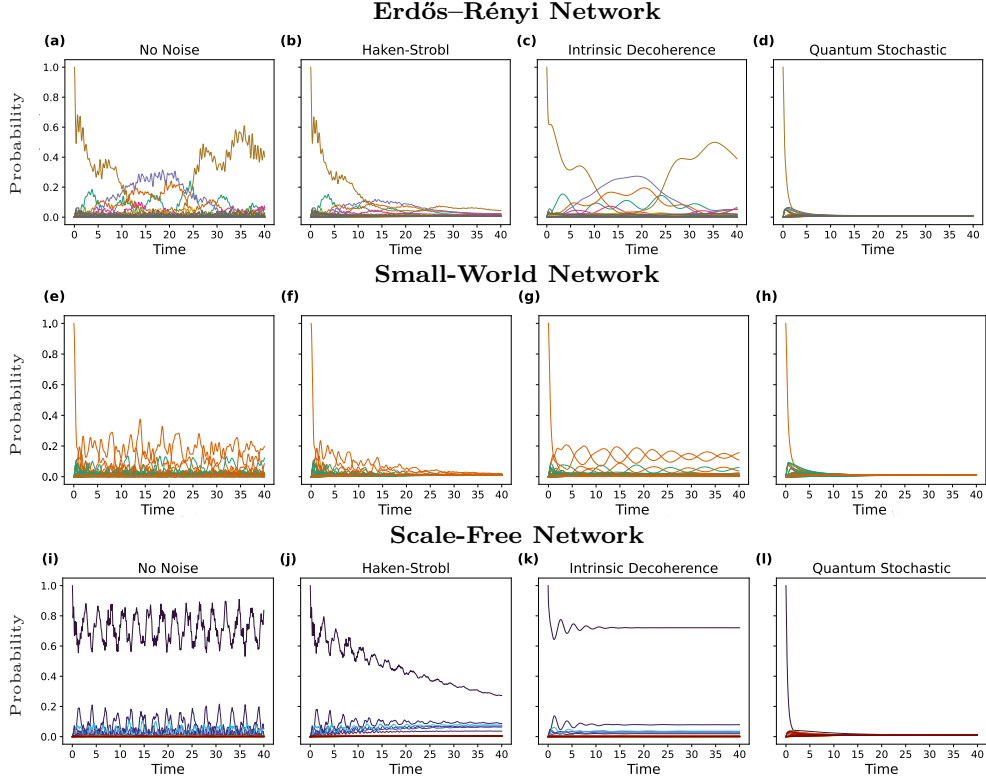


Fig. 4 Probability versus time plots on complex network topologies with network size $N = 100$ under various decoherence models. The top row shows the probability distribution of the CTQW on an Erdős-Rényi network, with the walker initially localized on a randomly selected node at time $t = 0$ (a)-(d). The middle row depicts the dynamics on a small-world network (e)-(h), while the bottom row presents the probability evolution on a scale-free network, where the walker is initially placed on a high-degree node (i)-(l). For each network, the probability distribution across all nodes is shown over time, with the occupation probability of each node represented using a distinct color.

Fig. 4 shows that the scale-free network exhibits distinct behavior compared to the Erdős-Rényi and small-world networks, particularly in the noiseless case, as illustrated in Fig. 4(a),(e),(i). Node centralities in scale-free networks vary significantly due to their inherently heterogeneous structure. As a result, the evolution of CTQW on such networks depends strongly on the centrality of the node where the walker is initially localized. For instance, when the initially localized node has the highest degree but not the highest closeness centrality, the occupation probabilities at the highest-degree and highest-closeness nodes exhibit an anti-phase synchronization pattern (see Appendix B Fig. 14). The probability amplitudes of anti-phase synchronized

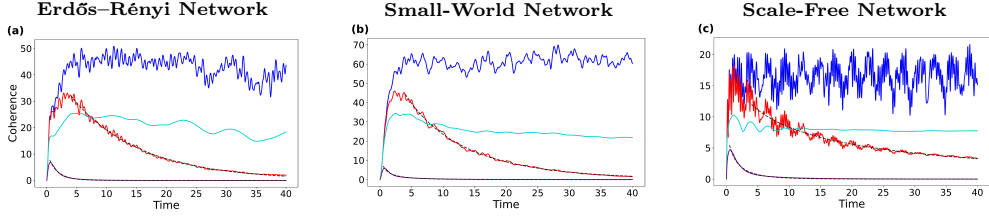


Fig. 5 Time evolution of the ℓ_1 -norm of coherence for complex network topologies with size $N = 100$. Coherence decay under Haken–Strobl noise and quantum stochastic walk (QSW) is modeled using the decay function given in Eq. (11), with best-fit parameters summarized in Table 2. The ℓ_1 -norm of coherence is plotted for the Erdős–Rényi network (a), small-world network (b), and scale-free network (c) under four conditions: no noise (blue), Haken–Strobl noise (red), intrinsic decoherence (cyan), and quantum stochastic walk (purple). These curves illustrate how coherence either diminishes or persists over time, depending on network structure and decoherence model.

nodes vary depending on the specific configuration of the network structure. Notably, strong localization at the initially occupied hub node is observed in heterogeneous networks, such as, the scale-free network Fig. 4(i) and star networks. This behavior is consistent with the previous study by Xu et al. [48] who showed that, in the thermodynamic limit ($\lim N \rightarrow \infty$), transition probabilities in star networks tend to remain localized at the initially localised site. In contrast, Erdős–Rényi and small-world networks lack pronounced degree heterogeneity and central hubs, leading to a more delocalized evolution of the CTQW. Interestingly, however, Fig. 5 shows that, in the absence of decoherence, both small-world and Erdős–Rényi networks maintain a higher ℓ_1 -norm of coherence compared to the scale-free network. This highlights the influence of network structure, suggesting that while hubs facilitate localization, they may simultaneously contribute to reduced coherence in noise-free conditions.

Under the influence of Haken–Strobl noise, the occupation probability at the initially localized node decays rapidly in both the Erdős–Rényi and small-world networks Fig. 4(b),(f), eventually leading to a uniform distribution. This renders the initially localized node indistinguishable from others, indicating complete delocalization across the network. In contrast, the scale-free network does not exhibit complete delocalization Fig. 4(j); although the occupation probability at the initially localized node decays over time, the distribution remains uneven, and the node probabilities do not converge to a uniform state.

Furthermore, we extracted the coherence decay coefficients λ and β (summarized in Table 2) by fitting the coherence data as shown in the red curves in Fig. 5 using Eq. (11). The red curves in Fig. 5(c) show that the scale-free network preserves quantum coherence for a longer duration under Haken–Strobl noise, as indicated by its relatively slow decay, indicated by a low β value.

In the presence of intrinsic decoherence, the CTQW exhibits partial localization at the initially localized node in the scale-free network Fig. 4(k), similar to the behavior observed in the noiseless case, but with a fixed probability. Localization behavior of CTQW is not observed in the Erdős–Rényi and small-world networks, as illustrated in Fig. 4(c),(g). Interestingly, the ℓ_1 -norm of coherence is not completely destroyed under intrinsic decoherence for any of the network topologies. This suggests that, despite

inducing partial localization in the scale-free network, intrinsic decoherence preserves quantum coherence across all topologies, ensuring stability for all topologies.

On the other hand, QSW dynamics lead to a complete delocalization of the quantum walker across all network types. As shown in Fig. 4(d),(h),(l), node probabilities tend to equalize, erasing the initial localization, particularly evident in the scale-free network, where the initial localization is entirely lost. Coherence analysis of λ and β from Table 2, and purple curves in Fig. 5 further shows that QSW induces the fastest coherence decay among all the decoherence models. Although Erdős-Rényi networks retain more coherence compared to other topologies under QSW, overall coherence degrades rapidly across all complex network topologies. However, this decay is not faster than exponential, as indicated by $\beta < 1$.

Decoherence	Network	λ	β
Haken-Strobl	Erdős-Rényi	0.10	0.84
	Small-World	0.17	0.96
	Scale-Free	0.24	0.37
Quantum Stochastic	Erdős-Rényi	0.71	0.45
	Small-World	1.53	0.90
	Scale-Free	0.96	0.62

Table 2 Coherence decay fitting parameters for Erdős-Rényi, small-world and scale-free under Haken-Strobl and QSW

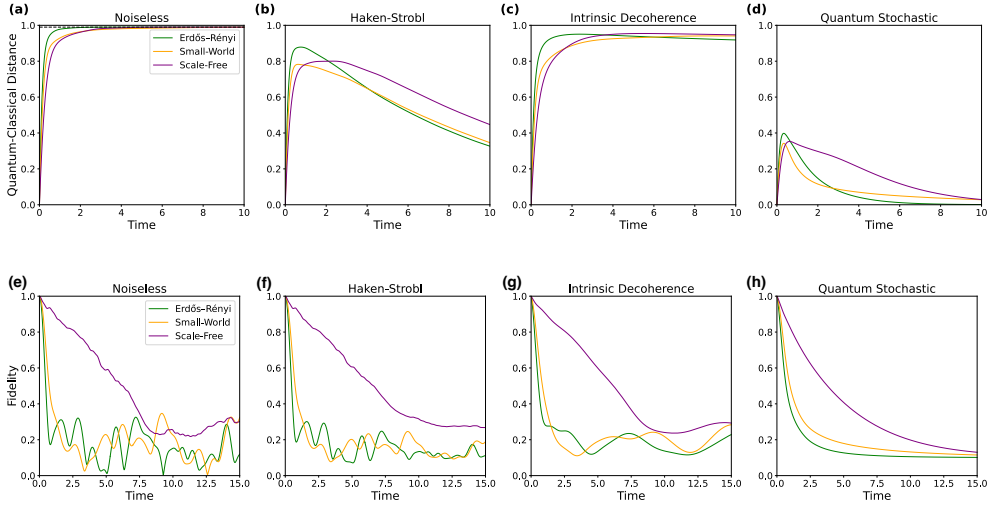


Fig. 6 Quantum-classical distance and fidelity with the initial state for complex network topologies with size $N = 100$. Quantum-classical distance and fidelity with the initial state for Erdős-Rényi (green), small-world (yellow), and scale-free (magenta) networks under the absence of noise (a),(e) and three decoherence models: Haken-Strobl (b),(f), intrinsic Decoherence (c),(g), and QSW (d),(h).

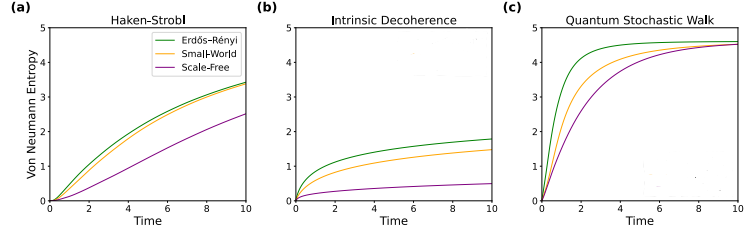


Fig. 7 Time evolution of von Neumann entropy for complex network topologies for size $N = 100$. Von Neumann entropy for Erdős-Rényi (green), small-world (yellow), and scale-free (magenta) networks under Haken-Strobl (a), Intrinsic Decoherence (b), and QSW (c).

Further to assess the system’s stability, we utilize a set of standard metrics from open quantum system analysis, such as quantum-classical distance, von Neumann entropy, and fidelity. The quantum-classical distance in Fig. 6(a)-(d) tells that the scale-free network exhibits greater resistance to classicalization under decoherence compared to the Erdős-Rényi and small world network, since as time progresses, scale-free has more quantum classical distance than other topologies underlying all decoherence dynamics. It maintains a significantly higher quantum-classical distance in the presence of both QSW and Haken-strobl both of which tend to classicalize the system over long timescales. For intrinsic decoherence in Fig. 6(c), the distance does not decay to zero, indicating that classicalization does not occur and quantum features are consistently preserved for all networks. For the noiseless scenario, across all network topologies, the quantum-classical distance converges to the theoretical value $\lim_{t \rightarrow \infty} D_{QC}(t) = 1 - \frac{1}{N}$ [37], as represented by the dashed line in Fig. 6(a).

The fidelity plots in Fig. 6(e)-(h) show that the scale-free network topology exhibits localization near the initial state since it has high fidelity with the initial state. Higher the fidelity lesser the evolved state has deviated from the initial state. On contrast, the Erdős-Rényi and small-world networks have a little less fidelity across various decoherences.

Von Neumann entropy plots Fig. 7(a)-(c) show that entropy is high for Erdős-Rényi in all decoherence. Entropy is least for scale-free in the case of Haken-Strobl and QSW, showing scale-free is not much deviated from the pure state as compared to Erdős-Rényi. This implies that scale-free is more resilient to all noises and Erdős-Rényi is more prone to mixed states than other topologies. For the noiseless case, the entropy always remains zero.

6 Conclusion

In this work, we investigate the stability of quantum systems by analyzing the dynamics of CTQWs on various network topologies under different decoherence mechanisms. We define stability in terms of the preservation of quantum properties over time and examine how this preservation is influenced by the interplay between network structure and decoherence model. To analyze this, we consider both simple network structures, including star, cycle, and complete graphs, and complex topologies such as Erdős-Rényi, small-world, and scale-free networks.

We evaluate the dynamics of CTQWs on these networks to examine the persistence of quantum properties, both in the absence of noise and under three decoherence models namely, Haken-Strobl, intrinsic decoherence and QSW. This systematic analysis allows us to explore how network structure and decoherence jointly influence CTQW stability. To quantify the stability, first we compute the node probability distribution of the quantum walker and the ℓ_1 -norm of coherence. In addition to these primary measures, we also use fidelity, quantum-classical distance, and von Neumann entropy measures for providing a comprehensive characterization of the preservation of quantum properties.

Based on these metrics, we find that stability varies significantly across decoherence models, for example intrinsic decoherence preserves coherence most effectively, followed by Haken-Strobl noise, while QSW result in the most rapid coherence loss. Our results reveal that coherence preservation depends not only on the type of decoherence but also on the underlying topology and the specific node at which the quantum walker is initialized.

Delving deeper, we observe that homogeneous networks such as the cycle exhibit high coherence in the absence of noise but are highly vulnerable under decoherence. In contrast, heterogeneous topologies like the star network demonstrate greater robustness under Haken-Strobl and intrinsic decoherence, as quantified by the ℓ_1 -norm of coherence. In the case of QSW, star networks initialized at peripheral nodes retain coherence longer and delay the onset of uniform probability distribution compared to central hub initialization. Interestingly, complete and star networks initialized at central nodes exhibit similar probability distributions and similar stability measures under decoherence, reflecting the impact of local connectivity due to comparable node degrees.

For complex networks, when coherence preservation is quantified using ℓ_1 -norm of coherence indicates that scale-free networks are the most stable under Haken-Strobl but exhibit slightly faster coherence decay than Erdős-Rényi networks under QSW dynamics. When stability is assessed using fidelity and von Neumann entropy, we observe distinct temporal behaviors across Erdős-Rényi, small-world, and scale-free networks. These results indicate that the increased heterogeneity of scale-free networks contributes to their enhanced stability. However, when using the quantum-classical distance as a stability measure, particularly under noiseless and intrinsic decoherence case, all network types yield nearly identical trajectories, making it difficult to distinguish relative stability. The interpretation of stability is inherently application-dependent. For example, high entropy may impair the efficiency of quantum search algorithms [50], while a large quantum-classical distance, indicating strong deviation from classical dynamics can benefit the design of optimized chiral quantum walks [51].

In general, heterogeneous networks exhibit greater coherence stability than homogeneous networks with less connectivity. Moreover, the stability of such networks is strongly influenced by the initialization of the quantum walker at high-degree nodes, which tends to promote localization and coherence retention under noise but reduces coherence in noiseless conditions. This observation highlights a fundamental trade-off between localization and coherence. The implications of this trade-off are particularly relevant for quantum information processing: coherence can serve as a resource for

quantum search algorithms based on quantum walks [52, 53], whereas high fidelity often indicative of localization can be exploited for robust quantum memories [54].

Based on our analysis, there is significant scope for future research on quantum coherence stability in noisy environments by investigating additional structural properties of networks and considering the dynamics of multiple continuous-time quantum walkers (multi-CTQWs).

Acknowledgments

ALJ acknowledges the University Grants Commission (UGC), India, for financial support. CM acknowledges support from the Anusandhan National Research Foundation (ANRF) India (Grants Numbers SRG/2023/001846 and EEQ/2023/001080).

A CTQW on Triangle Graph

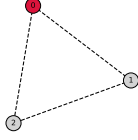


Fig. 8 Triangle graph with the initial localization of the CTQW at node 0.

For the triangle graph, we consider that the CTQW is localized at node 0, as illustrated in Fig. 8. The system's Hamiltonian is given by the graph Laplacian:

$$H = \begin{bmatrix} 2 & -1 & -1 \\ -1 & 2 & -1 \\ -1 & -1 & 2 \end{bmatrix} \quad (12)$$

In the noiseless case, the evolution of the density matrix is governed by the unitary transformation according to :

$$\rho(t) = e^{-iHt} \rho_0 e^{iHt} \quad (13)$$

For the triangle graph, this results in the following density matrix, derived analytically:

$$\rho_t = \frac{1}{9} \begin{bmatrix} 5 + 4 \cos 3t & -1 + 2e^{-3it} - e^{3it} & -1 + 2e^{-3it} - e^{3it} \\ -1 + 2e^{3it} - e^{-3it} & 2 - 2 \cos 3t & 2 - 2 \cos 3t \\ -1 + 2e^{3it} - e^{-3it} & 2 - 2 \cos 3t & 2 - 2 \cos 3t \end{bmatrix} \quad (14)$$

From Figs. 9(a),(e), we observe that the node occupation probabilities obtained from the theoretical denoted as a dashed line, match exactly with the occupation

probability extracted from the numerical density matrices, confirming the consistency between the analytical and simulation results.

As we know, the long-time behavior of node occupation probabilities serves as a reliable indicator of quantum stability. From Fig. 9, we observe that in the absence of decoherence, CTQWs on the triangle graph exhibits persistent oscillatory dynamics without reaching a steady probability distribution, reflecting sustained quantum behavior. In contrast, the introduction of decoherence drives the system toward a steady probability distribution, with the rate and nature of convergence depending critically on both the decoherence model and the network topology.

As shown in Fig. 9(b),(f), the presence of Haken–Strobl noise leads to damped oscillations in the node occupation probabilities, which gradually converge to a uniform distribution. This behavior closely resembles that of the QSW model, Fig. 9(d),(h), however, in the QSW, convergence is faster and smoother, with oscillations decaying over a shorter timescale. In contrast, under intrinsic decoherence, Fig. 9(c),(g), the occupation probabilities do not evolve toward uniformity. Instead, they stabilize at two distinct values, highlighting a fundamental difference in the asymptotic behavior across these decoherence models.

These observations indicate that, for the triangle graph, intrinsic decoherence tends to preserve quantum coherence more effectively than both the Haken–Strobl and quantum stochastic walk models. This underscores the critical role of the decoherence mechanism in shaping the long-term quantum dynamics of the system.

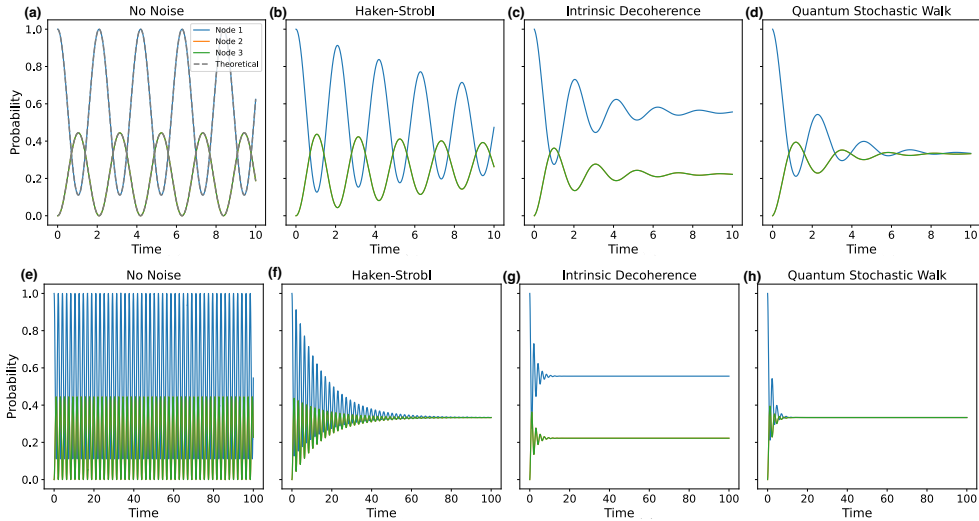


Fig. 9 Occupation probabilities for quantum walker in a triangle graph. The (a)-(d) shows the time evolution of the node occupation probabilities, with numerical results matching the analytically derived density matrix solutions (gray dashed lines). Nodes 2 and 3 exhibit identical probabilities, leading to overlapping curves. (e)-(h) presents the long-time occupation probabilities, using the same color scheme as in the top panels.

B CTQWs on Network Topologies ranging from Homogeneous to Heterogeneous structures

To further investigate which network structures are most effective in preserving quantum properties and supporting the stability of quantum systems, we analyze CTQWs on several network topologies, ranging from homogeneous structures such as the cycle graph to highly heterogeneous ones such as the star network. The objective is to identify topologies that offer the greatest stability in various decoherence models.

To investigate this, we calculate the quantum-classical distance, fidelity with the initial state, and von Neumann entropy for the cycle, star, complete, star, Erdős–Rényi, small-world and scale-free network topologies. Results for networks of size $N = 10$ are presented in Fig. 10(a)–(h) and Fig. 11(a)–(c), while results for network size $N = 50$ are shown in Fig. 12(a)–(h) and Fig. 13(a)–(c).

These figures show that simulations with larger network sizes reveal a clearer distinction in the dynamical behavior across different topologies. From these figures, we observe that for all decoherence models, except the QSW, the complete graph (red curves) and the star network (orange curves) with hub node initialization consistently demonstrate the highest stability. This is evidenced by their highest quantum-classical distance and fidelity with respect to the initial state, along with the lowest von Neumann entropy. These findings are consistent with earlier results based on the ℓ_1 -norm of coherence.

In contrast, the star network with peripheral node initialization tends to classicalize more rapidly, as indicated by its lowest quantum-classical distance, suggesting reduced stability. However this same configuration displays a higher fidelity with the initial state and lower entropy compared to other topologies. This highlights that different stability metrics capture distinct aspects of the CTQW’s stability in different topologies and are relevant in different contexts, as elaborated in the conclusion (Sec. 6). Additionally, under the QSW decoherence, the decay of ℓ_1 -norm of coherence is slower for this configuration as shown in Fig. 3(g), further emphasizing the intricate interplay between topology, initial conditions and the choice of stability measures.

Further analysis of Fig. 12 and Fig 13 reveals that, under both Haken–Strobl noise and intrinsic decoherence, the quantum-classical distance again identifies the complete graph and the star network with hub node initialization as the most stable configurations in all metrics. Surprisingly, despite being homogeneous, the cycle topology demonstrates the highest resilience to classicalization against the QSW decoherence. Among the remaining complex network structures, stability trends align with their degree of heterogeneity: scale-free networks exhibit higher stability than followed by small-world and Erdős–Rényi networks.

Overall, our results indicate that the star network, owing to its extreme structural heterogeneity, exhibits the highest level of quantum stability across a range of decoherence models. It is followed by the scale-free and small-world networks, which also benefit from structural heterogeneity and hub-like features. In contrast, homogeneous networks such as the cycle and Erdős–Rényi graphs, which lack prominent central nodes and have relatively low connectivity, are generally the least favorable for preserving quantum coherence, particularly under quantum stochastic noise. Notably, the

complete graph, despite its homogeneity, provides high stability due to its dense connectivity, enabling sustained coherence across the network. These findings highlight the crucial role of both heterogeneity and connectivity in determining a network's resilience to decoherence, with implications for the design of robust quantum systems.

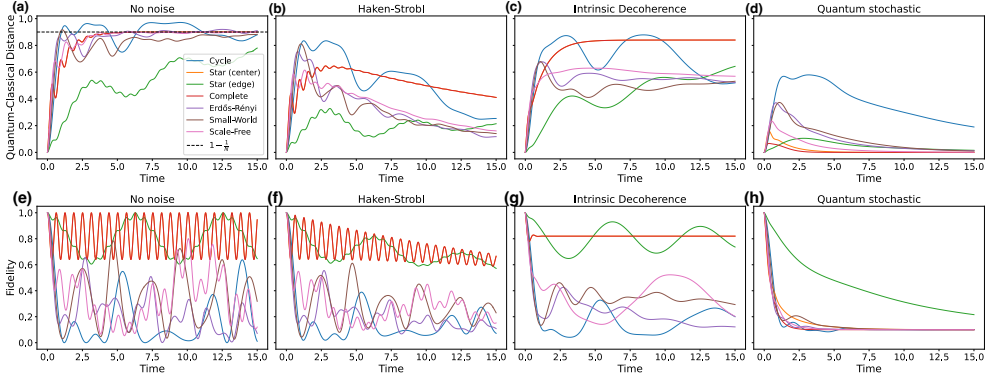


Fig. 10 Quantum-classical distance and fidelity with the initial state for Network size $N = 10$. Results are shown for different network topologies: cycle, star (with both central and peripheral node initialization), complete, Erdős-Rényi, small-world and scale-free networks (with hub node initialization) under both the noiseless evolution (a),(e) and three decoherence models: Haken-Strobl (b),(f), intrinsic decoherence (c),(g), and the QSW (d),(h).

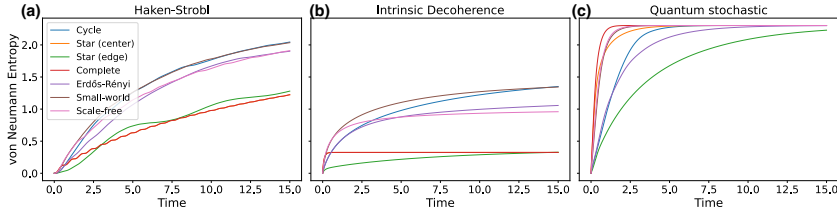


Fig. 11 Time evolution of von Neumann entropy for networks with size $N = 10$. Von Neumann entropy for all network topologies when the CTQW evolves under (a) Haken-Strobl noise, (b) intrinsic decoherence, and (c) QSW.

In scale-free networks, nodes often exhibit significant variability in centrality measures such as degree, closeness, and betweenness. We find that when the nodes with the highest degree and highest closeness centrality are distinct, the dynamics of the CTQW exhibit a striking anti-synchronization pattern. Specifically, when the walker is initialized on either the highest-degree node (Fig.14(a)) or the highest-closeness node (Fig.14(b)), the probability distributions over time show out-of-phase oscillations between these two nodes, suggesting a dynamical competition in occupation probabilities.

In contrast, when the highest-degree and highest-closeness centrality coincide at a single node, the walker remains strongly localized on the initial node throughout the

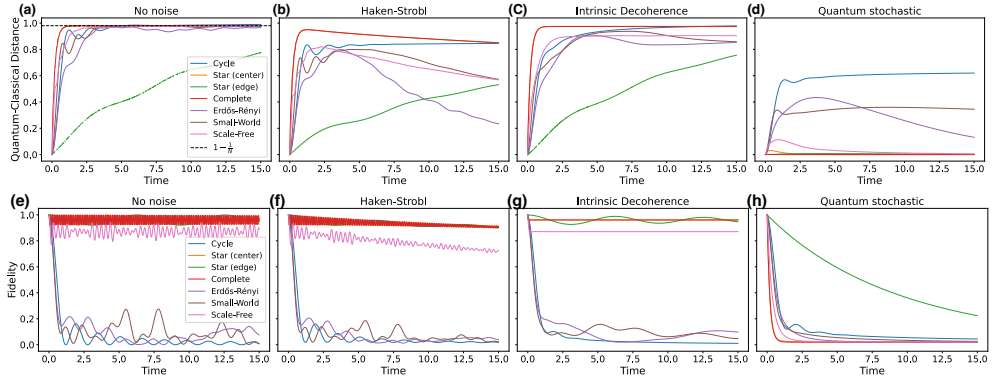


Fig. 12 Quantum-classical distance and fidelity with the initial state for different network topologies with network size $N = 50$. The quantum walker is evolved under the conditions: no noise (a),(e), Haken–Strobl noise (b),(f), intrinsic decoherence (c),(g), and the QSW (d),(h). In the quantum-classical distance plots, the gray dashed line for the noiseless case (a) corresponds to the analytical results.

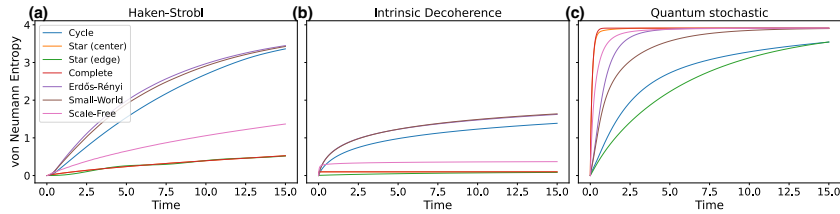


Fig. 13 Von Neumann entropy for Network size $N = 50$. The quantum walker is evolved under three conditions: Haken–Strobl noise (a), intrinsic decoherence (b), and the QSW (c).

evolution, as shown in Fig. 14(c). Even in the presence of Haken–Strobl decoherence, the decay of the occupation probability is significantly slower, indicating a pronounced robustness of localization that resists noise-induced spreading.

On the other hand, when the walker is initialized on the lowest-degree node (Fig. 14(d)), the CTQW exhibits no such localization behavior. The walker spreads more readily across the network, and the occupation probability of the initial node diminishes rapidly. Under quantum stochastic walk dynamics, the probability distribution in this case reaches equilibration more slowly compared to scenarios involving high-degree or high-closeness nodes. These findings underscore the critical role of node centrality in shaping both coherence preservation and transport behavior in heterogeneous quantum networks.

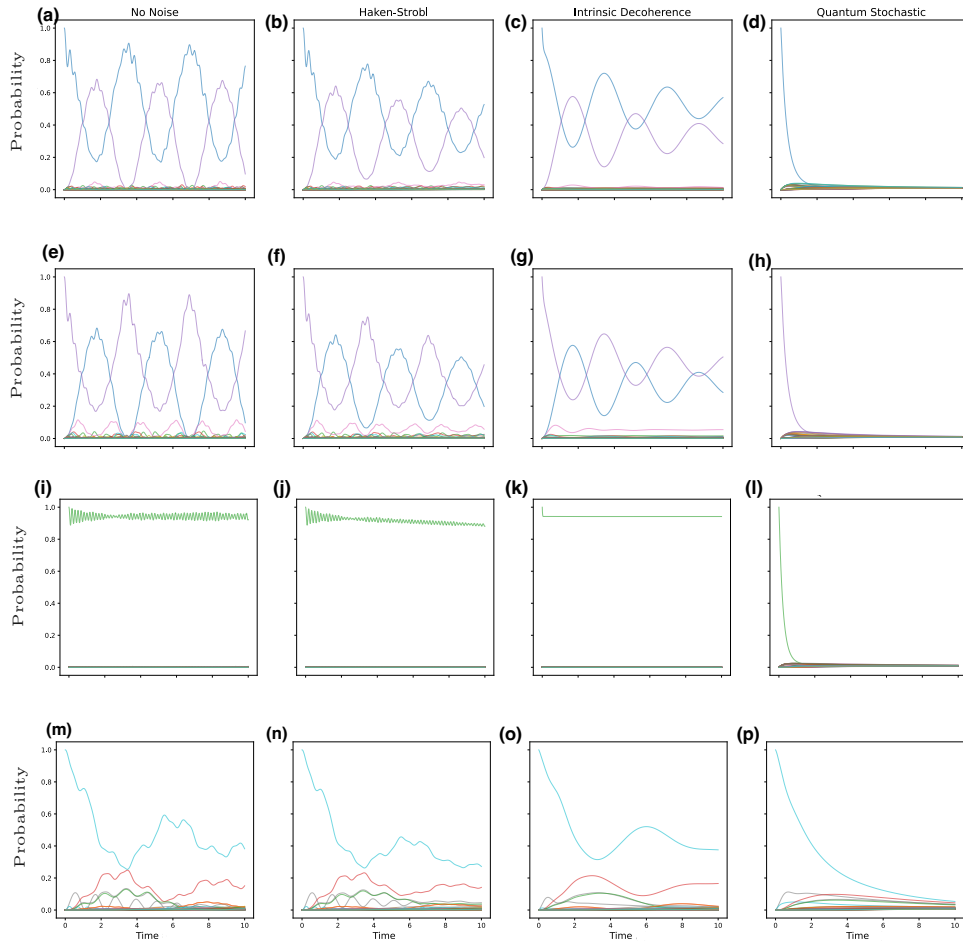


Fig. 14 Node occupation probability versus time under different initial conditions of scale-free networks with size $N = 100$ (a)–(d): The network structure has distinct nodes for the highest degree and highest closeness centrality. The walker is initially localized on the highest-degree node, which exhibits anti-synchronization with highest-closeness node. (e)–(h): Similar network configuration as above, but the walker is initially localized on the highest-closeness node. anti-synchronization is observed with the highest-degree node in this case. (i)–(l): The walker starts at a node where both the highest degree and highest closeness centralities coincide. (m)–(p): The walker is initialized on the lowest-degree node.

References

- [1] Y. Aharonov, L. Davidovich, N. Zagury, Quantum random walks. *Physical Review A* **48**(2), 1687 (1993)
- [2] A. Ambainis, Quantum walks and their algorithmic applications. *International Journal of Quantum Information* **1**(04), 507–518 (2003)
- [3] N. Konno, Quantum walks. *Lecture notes in mathematics* **1954**, 309–452 (2008)
- [4] A.M. Childs, J. Goldstone, Spatial search by quantum walk. *Physical Review A—Atomic, Molecular, and Optical Physics* **70**(2), 022314 (2004)
- [5] E. Farhi, S. Gutmann, Quantum computation and decision trees. *Physical Review A* **58**(2), 915 (1998)
- [6] M.N. Jayakody, C. Meena, P. Pradhan, Revisiting one-dimensional discrete-time quantum walks with general coin. *Physics Open* **17**, 100189 (2023)
- [7] A.M. Childs, Universal computation by quantum walk. *Physical review letters* **102**(18), 180501 (2009)
- [8] O. Boada, A. Celi, J. Rodríguez-Laguna, J.I. Latorre, M. Lewenstein, Quantum simulation of non-trivial topology. *New Journal of Physics* **17**(4), 045007 (2015). <https://doi.org/10.1088/1367-2630/17/4/045007>
- [9] S. Chakraborty, L. Novo, A. Ambainis, Y. Omar, Spatial search by quantum walk is optimal for almost all graphs. *Physical review letters* **116**(10), 100501 (2016)
- [10] S. Apers, S. Chakraborty, L. Novo, J. Roland, Quadratic speedup for spatial search by continuous-time quantum walk. *Physical review letters* **129**(16), 160502 (2022)
- [11] G. Coutinho, K. Guo, V. Schmeits, Peak state transfer in continuous quantum walks. *arXiv preprint arXiv:2505.11986* (2025)
- [12] U. Sağlam, M. Paternostro, Ö.E. Müstecaplıoğlu, Entanglement transfer via chiral and continuous-time quantum walks on a triangular chain. *Physica A: Statistical Mechanics and its Applications* **612**, 128480 (2023)
- [13] M. Mohseni, P. Rebentrost, S. Lloyd, A. Aspuru-Guzik, Environment-assisted quantum walks in photosynthetic energy transfer. *The Journal of chemical physics* **129**(17) (2008)
- [14] C.H. Ren, Y.M. Lai, T.Q. Song, Decoherence of an open system under continuous quantum measurement of energy. *International Journal of Theoretical Physics* **48**, 2081–2087 (2009)

- [15] C. Benedetti, F. Buscemi, P. Bordone, M.G. Paris, Non-markovian continuous-time quantum walks on lattices with dynamical noise. *Physical Review A* **93**(4), 042313 (2016)
- [16] F. Caruso, A.W. Chin, A. Datta, S.F. Huelga, M.B. Plenio, Highly efficient energy excitation transfer in light-harvesting complexes: The fundamental role of noise-assisted transport. *The Journal of Chemical Physics* **131**(10) (2009)
- [17] M.B. Plenio, S.F. Huelga, Dephasing-assisted transport: quantum networks and biomolecules. *New Journal of Physics* **10**(11), 113019 (2008). <https://doi.org/10.1088/1367-2630/10/11/113019>
- [18] G. Milburn, Intrinsic decoherence in quantum mechanics. *Physical Review A* **44**(9), 5401 (1991)
- [19] H. Haken, G. Strobl, An exactly solvable model for coherent and incoherent exciton motion. *Zeitschrift für Physik A Hadrons and nuclei* **262**(2), 135–148 (1973)
- [20] F. Caruso, Universally optimal noisy quantum walks on complex networks. *New Journal of Physics* **16**(5), 055015 (2014). <https://doi.org/10.1088/1367-2630/16/5/055015>
- [21] G. Bressanini, C. Benedetti, M.G. Paris, Decoherence and classicalization of continuous-time quantum walks on graphs. *Quantum Information Processing* **21**(9), 317 (2022)
- [22] F.W. Strauch, Reexamination of decoherence in quantum walks on the hypercube. *Physical Review A—Atomic, Molecular, and Optical Physics* **79**(3), 032319 (2009)
- [23] I. Siloi, C. Benedetti, E. Piccinini, J. Piilo, S. Maniscalco, M.G. Paris, P. Bordone, Noisy quantum walks of two indistinguishable interacting particles. *Physical Review A* **95**(2), 022106 (2017)
- [24] C. Benedetti, F. Buscemi, P. Bordone, Quantum correlations in continuous-time quantum walks of two indistinguishable particles. *Physical Review A—Atomic, Molecular, and Optical Physics* **85**(4), 042314 (2012)
- [25] O. Mülken, A. Blumen, Continuous-time quantum walks: Models for coherent transport on complex networks. *Physics Reports* **502**(2-3), 37–87 (2011)
- [26] D.I. Tsomokos, Quantum walks on complex networks with connection instabilities and community structure. *Physical Review A—Atomic, Molecular, and Optical Physics* **83**(5), 052315 (2011)

- [27] S. Boccaletti, V. Latora, Y. Moreno, M. Chavez, D.U. Hwang, Complex networks: Structure and dynamics. *Physics reports* **424**(4-5), 175–308 (2006)
- [28] C. Meena, C. Hens, S. Acharyya, S. Haber, S. Boccaletti, B. Barzel, Emergent stability in complex network dynamics. *Nature Physics* **19**(7), 1033–1042 (2023)
- [29] P.D. Rungta, C. Meena, S. Sinha, Identifying nodal properties that are crucial for the dynamical robustness of multistable networks. *Physical Review E* **98**(2), 022314 (2018)
- [30] C. Meena, P.D. Rungta, S. Sinha, Threshold-activated transport stabilizes chaotic populations to steady states. *Plos one* **12**(8), e0183251 (2017)
- [31] L. Böttcher, M.A. Porter, Classical and quantum random-walk centrality measures in multilayer networks. *SIAM Journal on Applied Mathematics* **81**(6), 2704–2724 (2021). <https://doi.org/10.1137/20M1385998>
- [32] S. Bose, Quantum communication through spin chain dynamics: an introductory overview. *Contemporary Physics* **48**(1), 13–30 (2007)
- [33] H.P. Breuer, F. Petruccione, *The theory of open quantum systems* (Oxford University Press, USA, 2002)
- [34] A. Kossakowski, On quantum statistical mechanics of non-hamiltonian systems. *Reports on Mathematical Physics* **3**(4), 247–274 (1972)
- [35] G. Lindblad, On the generators of quantum dynamical semigroups. *Communications in mathematical physics* **48**, 119–130 (1976)
- [36] V. Gorini, A. Kossakowski, E.C.G. Sudarshan, Completely positive dynamical semigroups of n-level systems. *Journal of Mathematical Physics* **17**(5), 821–825 (1976)
- [37] V. Gultieri, C. Benedetti, M.G. Paris, Quantum-classical dynamical distance and quantumness of quantum walks. *Physical Review A* **102**(1), 012201 (2020)
- [38] A.L. Barabási, R. Albert, Emergence of scaling in random networks. *science* **286**(5439), 509–512 (1999). <https://doi.org/10.1126/science.286.5439.509>
- [39] P. Erdős, A. Rényi, et al., On the evolution of random graphs. *Publ. math. inst. hung. acad. sci* **5**(1), 17–60 (1960)
- [40] D.J. Watts, S.H. Strogatz, Collective dynamics of ‘small-world’ networks. *nature* **393**(6684), 440–442 (1998)
- [41] O. Mülken, V. Pernice, A. Blumen, Quantum transport on small-world networks: A continuous-time quantum walk approach. *Physical Review E—Statistical, Nonlinear, and Soft Matter Physics* **76**(5), 051125 (2007)

- [42] T. Baumgratz, M. Cramer, M.B. Plenio, Quantifying coherence. *Physical review letters* **113**(14), 140401 (2014)
- [43] R. Jozsa, Fidelity for mixed quantum states. *Journal of modern optics* **41**(12), 2315–2323 (1994)
- [44] M. Raginsky, A fidelity measure for quantum channels. *Physics Letters A* **290**(1-2), 11–18 (2001)
- [45] A. Gilchrist, N.K. Langford, M.A. Nielsen, Distance measures to compare real and ideal quantum processes. *Physical Review A—Atomic, Molecular, and Optical Physics* **71**(6), 062310 (2005)
- [46] H.B. Chen, C. Gneiting, P.Y. Lo, Y.N. Chen, F. Nori, Simulating open quantum systems with hamiltonian ensembles and the nonclassicality of the dynamics. *Physical review letters* **120**(3), 030403 (2018)
- [47] E.G. Rieffel, W.H. Polak, *Quantum computing: A gentle introduction* (MIT press, 2011)
- [48] X.P. Xu, Exact analytical results for quantum walks on star graphs. *Journal of Physics A: Mathematical and Theoretical* **42**(11), 115205 (2009). <https://doi.org/10.1088/1751-8113/42/11/115205>
- [49] R. Kohlrausch, Theorie des elektrischen rückstandes in der leidener flasche. *Annalen der Physik* **167**(2), 179–214 (1854). <https://doi.org/10.1002/andp.18541670103>
- [50] S. Bose, L. Rallan, V. Vedral, Communication capacity of quantum computation. *Physical Review Letters* **85**(25), 5448 (2000)
- [51] M. Frigerio, C. Benedetti, S. Olivares, M.G. Paris, Quantum-classical distance as a tool to design optimal chiral quantum walks. *Physical Review A* **105**(3), 032425 (2022)
- [52] H.L. Shi, S.Y. Liu, X.H. Wang, W.L. Yang, Z.Y. Yang, H. Fan, Coherence depletion in the grover quantum search algorithm. *Physical Review A* **95**(3), 032307 (2017)
- [53] Y.L. Su, S.Y. Liu, X.H. Wang, H. Fan, W.L. Yang, Coherence as resource in scattering quantum walk search on complete graph. *Scientific Reports* **8**(1), 11081 (2018)
- [54] C.M. Chandrashekar, T. Busch, Localized quantum walks as secured quantum memory. *Europhysics Letters* **110**(1), 10005 (2015). <https://doi.org/10.1209/0295-5075/110/10005>